Theor Appl Climatol (2015) 119:379–389
DOI 10.1007/s00704-014-1114-2

ORIGINAL PAPER

Toward a record of Central Pacific El Niño events since 1880

M. Pascolini-Campbell · D. Zanchettin · O. Bothe · C. Timmreck · D. Matei · J. H. Jungclaus · H.-F. Graf

Received: 4 April 2013 / Accepted: 28 January 2014 / Published online: 28 February 2014

Abstract We investigate the various methods currently available for distinguishing between the Central Pacific (CP) El Niño (or "El Niño Modoki") and the canonical El Niño by considering nine different methods and five sea surface temperature (SST) datasets from 1880 to 2010. This is aimed to demonstrate the variety which exists between different classification methods as well as to help identify years which can be more confidently classified as CP events. Classifying CP El Niños based on the greatest convergence between methods and between SST datasets provides a more robust identification of these events. Analysis of the SST patterns of the CP years identified demonstrates several misclassifications, stressing the importance of not relying solely on indices. After removal, 14 years which are classified the most consistently as CP events include the following: 1885/1886, 1914/1915, 1940/1941, 1958/1959, 1963/1964, 1968/1969, 1977/1978, 1986/1987, 1990/1991, 1991/1992, 1994/1995, 2002/2003, 2003/2004, and 2004/2005. Our findings also indicate the intermittent appearance of CP events throughout the time period investigated, inciting the role of multidecadal natural climate variability in generating CP El Niños.

M. Pascolini-Campbell (✉)
Department of Earth and Environmental Sciences, Columbia University, New York, NY, USA
e-mail: madeleine.pascolini@gmail.com

M. Pascolini-Campbell · D. Zanchettin · C. Timmreck · D. Matei · J. H. Jungclaus
Max Planck Institute for Meteorology, Hamburg, Germany

O. Bothe
Leibniz Institute of Atmospheric Physics, at the University of Rostock, Kühlungsborn, Germany

H.-F. Graf
University of Cambridge, Cambridge, UK

1 Introduction

El Niño is the oceanic component of the El Niño-Southern Oscillation (ENSO), a phenomenon of large-scale variability in the coupled ocean-atmosphere system, originating over the tropical Pacific (Walker 1923, 1924). ENSO comprises the strongest climatic signal on interannual time scales and produces significant implications on the world's climate (Alexander et al. 2002). While the canonical El Niño involves the westward propagation of positive sea surface temperature anomalies (SSTAs) off the South American coast in the Eastern Pacific (Rasmusson and Carpenter 1982), in recent decades, a "new" type has been observed to be characterized by SSTAs confined to the Central Pacific (Kao and Yu 2009). It appears in the literature under a number of labels including "El Niño Modoki" (Ashok et al. 2007), "Central Pacific" (Kao and Yu 2009), "warm pool" (Kug et al. 2009), "Date Line El Niño" (Larkin and Harrison 2005) as well as "S-Mode" (Guilyardi 2006). Studies have also demonstrated that this new type (hereafter Central Pacific (CP) El Niño) may produce climatic teleconnections differing from the canonical El Niño (hereafter Eastern Pacific (EP) El Niño) thereby motivating research on the topic (Larkin and Harrison 2005; Ashok et al. 2007; Feng et al. 2010; Graf and Zanchettin 2012).

The discovery of the CP El Niño pattern of SST warming has encouraged considerable scientific research to distinguish it from the canonical event. The National Oceanic and Atmospheric Administration (NOAA) Climate Prediction Center (CPC) traditionally defines El Niños using the Niño 3.4 SST index (http://www.cpc.ncep.noaa.gov/data/indices/sstoi.indices) (covering the region between 170°W to 120°E and 5°N to 5°S) which must exceed 0.5 °C for five consecutive 3-month overlapping seasons (Trenberth 1997). The distinguished characteristics of the CP El Niño, in particular the confinement of anomalies to the Central Pacific, could not be adequately described by the Niño 3.4 index, leading to the construction of the "Trans-Niño Index" to encompass this variability (Trenberth and Stepaniak 2001). Further work culminated in a plethora of indices, methods, datasets,

and time periods used to identify CP El Niños (Ashok et al. 2007; Hendon et al. 2009; Kao and Yu 2009; Kim et al. 2009; Kug et al. 2009; Yeh et al. 2009; Yu and Kim 2010; Ren and Jin 2011). The result is a fairly varied delineation of the CP El Niño years, characteristics, climatological impacts, and mechanisms.

The prevalence and future evolution of the CP El Niño (particularly in light of climate change) is also currently under debate in the literature. Satellite evidence suggests that the frequency of CP events has increased in recent decades (Lee and McPhaden 2010). A climate modeling exploration also indicated the potential increase in frequency of CP El Niños with anthropogenic climate change (Yeh et al. 2009). Other studies contest these claims and suggest that CP El Niños can be explained by natural climate variability (Newman et al. 2011; McPhaden et al. 2011; Yeh et al. 2011). Different statistical analyses of SST datasets covering the past ~50 years help substantiate such claims through demonstrating that no significant changes have occurred in the distribution of CP and EP events (Nicholls 2008; L'Heureux et al. 2012).

The physical mechanisms responsible for the different patterns, and whether the two events are indeed different, are also disputed. Several studies have argued that the CP events comprise distinct climatic phenomena (Larkin and Harrison 2005; Ashok et al. 2007; Kao and Yu 2009; Kug et al. 2009). Other studies have raised doubts on CP uniqueness due to the statistical methods employed to characterize the events, particularly the use of empirical orthogonal functions (EOFs) (Lian and Chen 2012). The variable representation of CP and EP events in a multimodel ensemble (Guilyardi 2006) as well as in CMIP5 models (Kim and Yu 2012) also illustrates the limited understanding of the phenomenon. Studies of this nature are, however, limited by the variable classification of the CP event as well as by the sometimes limited quality of the available datasets. Giese and Ray (2011) note, for instance, the limited correlation of the location of El Niño events between the Hadley Center sea ice and SST (HadISST) dataset and the SODA reanalysis prior to 1950. The discrepancies between the classification of El Niño's amplitude and location between reconstructions and reanalyses is also found to exhibit greater differences in the first half of the twentieth century (Ray and Giese 2012).

The present study is aimed at demonstrating the variability which currently exists in the classification of CP El Niño years through considering multiple methods and SST datasets from 1880 to 2010. Motivation stems from the currently large span of techniques existing in the literature which have resulted in varied interpretations of the CP El Niño. Key questions addressed will include: How does the classification of the CP event differ when different techniques and datasets are used? Which years contain the greatest probability of a CP event having occurred? Has the occurrence of CP events changed in the time period investigated? This study also aims to demonstrate which years are classified as the most consistent CP events. It is hoped that this will help provide a more robust identification of CP events to assist with studies related to improving our understanding of the phenomenon.

2 Data and methodology

Nine methods for classifying the CP El Niño using different indices, datasets, and time periods are examined in the literature (summarized in Table 1). In particular, the EOF-based indices used by Takahashi et al. (2011) to classify CP and EP events can be approximated by the definitions of E and C indices (Table 1). The E index explains most of the variability in the Eastern Pacific east of 120°W and along the coast of Peru. The C index has its strongest explained variance in the Central Pacific (170°E to 100°W) and is therefore very close to the standard Niño 4 index. Time series of the 10-year running mean of different El Niño indices are computed to investigate whether dynamical changes in ENSO behavior can also be observed in long-term variability. In particular, the C and E indices are compared with the El Niño Modoki (EMI) index (Ashok et al. 2007) to examine their co-variability.

To investigate the comparability between the techniques, the classification criteria are applied to five different monthly SST datasets for the period 1880 to 2010. These include the NOAA Extended Reconstructed SST V2 (ERSST V2) (2°×2° global grid) (Smith and Reynolds 2004) and V3 (ERSST V3) (2°×2° global grid) (Smith et al. 2008), the HadISST (1°×1° global grid) (Rayner et al. 2003), the International Comprehensive Ocean-Atmosphere Data Set (ICOADS) 2° (2°×2° global grid) (Worley et al. 2005), and the Kaplan Extended SST V2 (5°×5° global grid) (Kaplan et al. 1998). Data are preprocessed to give deseasonalized monthly SSTAs, using 1880 to 2010 as the base period to compute the anomalies. Time series of the indices used by the different authors are created for each dataset. The SST datasets are not detrended.

The classifications are performed for each of the five datasets and nine methods, and the number of CP El Niños classified for each year is recorded. Classified years represent the CP events with mature phases in December and extending into the following year. Indices are here evaluated based on all available data, without filling missing values. Of course, this is a significant caveat for our interpretation of the results. Poor quality and sparse SST observations are noted, in particular, for the early part of the twentieth century in the datasets used. Limitations due to the incomplete nature of the data are especially evident in the ICOADS dataset, which suffers from missing values, especially in the early decades which appear in the different indices used in the classifications. We also note that problems may exist in classification across the different datasets due to discrepancies between reconstructions and reanalyses (Deser et al. 2010).

The results of the classification are then used to create a list of years which can be classified as CP events with greater

Table 1 Dataset, time period, indices, and criteria used to classify the CP El Niño

Author	Dataset	Time period	SST indices used	Criteria for defining CP event
Ashok et al. (2007)	HadISST	1958–2005	EMI	EMI>0.7 seasonal σ persisting for three seasons from boreal summer to winter
Hendon et al. (2009)	HadISST	1980–2006	EMI	EMI (3-month running mean) >0.7 seasonal standard deviation (SON)
Kao and Yu (2009)	HadISST	1950–2007	PC1 of SSTAs with subtracted anomalies regressed with Niño 1+2	SST PC1 >1 σ for more than 3 consecutive months
Kim et al. (2009)	ERSST V2	1950–2006	Niño 3 Niño 4	Niño 4>1 σ, Niño 3<1 σ (ASO)
Kug et al. (2009)	ERSST V2	1970–2005	Niño 3 Niño 4	Niño 4>Niño 3 and Niño 4>σ (SONDJF)
Ren and Jin (2011)	CPC NOAA time series	1950–2010	"Niño–warm pool" (WP)	WP>1 σ
Takahashi et al. (2011)	HadISST	1950–2009	*C* and *E* index	*C* or *E* index 5-month running mean>0.5 °C
Yeh et al. (2009)	ERSST V2	1979–2007	Niño 3 Niño 4	Niño 4>Niño 3 (DJF)
Yu and Kim (2010)	ERSST V3 and HadISST	1958–2007	PC1 of SSTAs with subtracted anomalies regressed with Niño 1+2	SST PC1 >1 σ (SONDJF)

Seasons are indicated in parentheses with the first letter of each month. "σ" is the standard deviation. The various indices are created using area-averaged values of SSTA. The EMI index is created through other Niño indices and defined as $EMI=SSTA_a-0.5\times SSTA_b-0.5\times SSTA_c$ ($SSTA_a$=165°E–140°W, 10°S–10°N; $SSTA_b$=110°W–70°W, 15°S–5°N; $SSTA_c$=125°E–145°E, 10°S–20°N). The *C* index is defined as $C=1.7\times$Niño 4$-0.1\times$Niño 1+2. The *E* index is defined as E=Niño 1+2$-0.5\times$Niño 4. The warm pool index is defined as WP=N3$-\alpha$N4 where N3=Niño 3, N4=Niño 4, and α=2/5 when N3×N4>0 and otherwise α=0. The other indices are defined as follows: Niño 4=160°E–150°W, 5°S–5°N; Niño 3=90°W–150°W, 5°S–5°N; Niño 1+2=90°W–80°W, 0°–10°S (Trenberth 1997). PC1 is the principal component of the leading empirical orthogonal function calculated from monthly SSTAs in the equatorial Pacific domain bounded by 10°N–10°S and 120°E–90°W

confidence. This is achieved by first identifying those years which are classified as the most consistent CP events among the different methods and datasets. The evolution of SSTA patterns of these individual years is then further investigated by using the HadISST dataset. Visual interpretation is supported by a grid cell-weighted pattern correlation analysis performed on December-January-February (DJF) data for the Pacific region within the domain (10°N–10°S; 120–280°*E*). Specifically, the following statistics is calculated for each candidate CP event: $R=\Sigma_i(w_iX_iX_{ei})/(\Sigma_i w_i)\sigma\sigma_e$ where Σ_i is the sum operator performed along grid point i, w_i is ith entry of the array of grid cell weights (corresponding to the area of each grid cell), X_i is the ith entry of the array of gridded SSTA of the selected candidate event with associated weighted standard deviation σ, and X_{ei} is the ith entry of the array of composite gridded SSTA of all CP candidate events with associated weighted standard deviation σ_e. Values of the *R* statistics close to 1 are associated to CP events whose DJF SSTA pattern more closely resembles our expectation for a typical CP event. Hence, visual investigation and the *R* statistics indicate which of the events can be classified as CP with the greatest robustness. These latter steps are to ensure that the indices have correctly identified CP events.

3 Results

Figure 1 summarizes the long-term evolution of the tropical Pacific SSTA indices for each considered dataset (ICOADS excluded), in the form of standardized 10-year running mean data. The 10-year running mean also helps to provide an indication of the low frequency variability of Pacific SSTAs over the period in the different regions considered. This is important to contextualize, based on the background state of Pacific SSTs, the CP events individuated in the subsequent analysis. The figure further illustrates the variability which exists between the indices and datasets used to classify the CP events. Differences among datasets are clearly visible early in the time period. An example is the pronounced negative value of the indices between 1895 and 1900 which appears in the HadISST and Kaplan SST, but not the ERSST datasets. The *C* index (see Table 1) is strongly correlated with the Niño 4 index (Pearson's *r* is >0.99 in the HadISST dataset) and is therefore not included in the figure. Correlations between the different indices are also investigated in the HadISST data for 30-year running means. The results indicate no correlation between *C* and EMI, r=0.93 between *C* and warm pool (WP) and r=0.10 between EMI and WP (note that this is only partly due to the different trends in the *C*, WP, and EMI series).

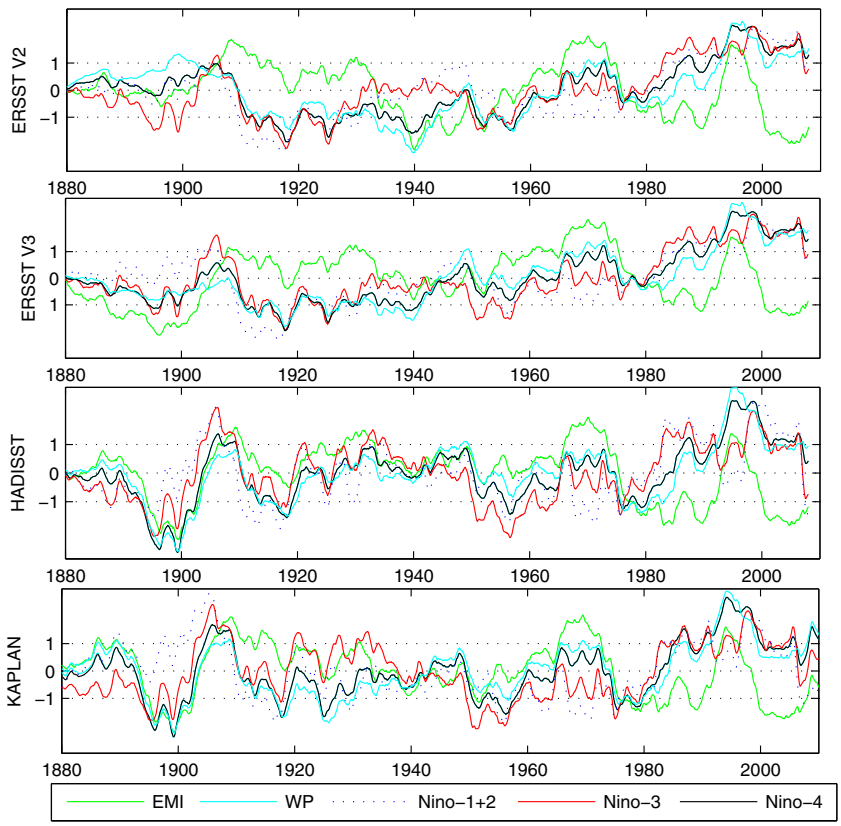

Fig. 1 Temporal evolution of the SSTA indices used to classify CP events for ERSST V2 (*a*), ERSST V3 (*b*), HadISST (*c*), and Kaplan (*d*). The ICOADS data are excluded due to the missing data earlier in the century. Plotted data are standardized, 10-year running mean-averaged indices. *Dotted lines* indicate the ±1 standard deviation band

Higher running means of the Niño 4 index than the Niño 1+2 index, for example, highlight likely periods of higher CP occurrence. Generally, we find a strong co-variability in all Niño indices at higher CP frequency, indicating basin-wide strong events appearing in the 10-year running means. These are coherent throughout all datasets. Stronger co-variability can be found for Niño 3 and Niño 4 indices, which, however, also exhibit differences indicated by periods of Niño 4> Niño 3 (indicating greater SSTAs further west in the Pacific) and vice versa. In the HadISST dataset, the 10-year running mean of Niño 3 and Niño 4 indices is correlated at r=0.79.

Two features are most striking in all datasets: (1) the strong decadal variability between 1890 and 1920 with a swing between strongly negative (1895–1902) and positive (1904–1910) and, afterwards, again negative indices and (2) since around 1980, all Niño indices except the EMI increase coherently, indicating a warming trend of the Pacific basin with the increase being strongest for Niño 4. It is also interesting to note the difference of the EMI index from 1990 to present in all datasets.

Figure 2 shows 10-year running means of the standardized E and C indices which suggest a period of preferred EP occurrence early in the time series, from approximately 1890 to 1910 in all datasets excluding ERSST V2. This is then replaced by a sub-decadal period of likely preferred CP occurrence starting around 1905 which is then seen to fall around 1910. Other periods of preferred CP occurrence distinct from EP occurrence are found around 1970 and, again, in the 1990s. These features are visible in all datasets and match our findings for the standard Niño indices discussed above. Again, however, we find substantial differences in the amplitudes between the datasets.

Figure 2 also shows the 10-year running mean of the EMI index of Ashok et al. (2007), which is equivalent to the PC2 of tropical Pacific SST variability. Despite the strong co-variability with the C index, without considering the time-persistence constraint of considering the magnitude of the EMI over three seasons in relation to the seasonal standard deviation (see Table 1), the index alone does not demonstrate the SST-associated CP warming during 1990 to present. Another feature of the EMI index which is illustrated in Fig. 2 is its ability to define periods in which C is greater than E and vice versa (for example, the period of negative C around 1900 and positive C around 1970). It is noted that the most recent period of high CP frequency from around 1995 to present is accompanied by a similarly high value in the E index.

Figure 3(a) illustrates the variability which exists between the methods used for classifying CP El Niños according to the dataset. Differences are to be expected given the range of indices and criteria employed by the different authors

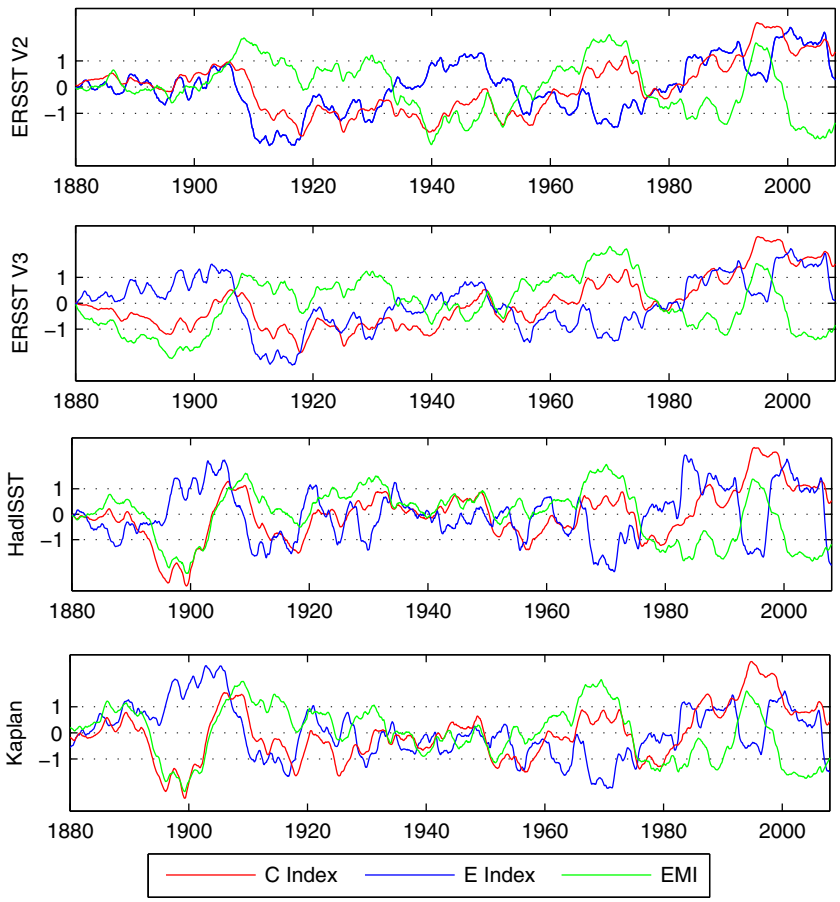

Fig. 2 Temporal evolution of the *C* and *E* indices (Takahashi et al. 2011) used to classify CP and EP events, respectively, and the EMI index (Ashok et al. 2007) used to classify CP for ERSST V2 (*a*), ERSST V3 (*b*), HadISST (*c*), and Kaplan (*d*). The ICOADS data are excluded due to the missing data earlier in the century. Plotted data are standardized, 10-year running mean-averaged indices. *Dotted lines* indicate the ±1 standard deviation band

(compare also Figs. 1 and 2). A key feature is the detection of CP El Niños already in the nineteenth century and early in the twentieth century. The CP events persist throughout the time series, despite variations and an increased event concentration in more recent decades.

Figure 3(b) illustrates the variability existing between the datasets used to classify CP El Niños according to the method. The results in Fig. 3(b) also display the incidence of CP events early in the dataset, although an agreement in their classification appears to increase in the later part of the twentieth century. The concentration of CP events is observed to increase later in the time period. In particular, Kug et al. (2009), Ren and Jin (2011), and Yeh et al. (2009) classify fewer CP events in the early portion of the data compared to the other methods. These three methods base their classification on the use of the Niño 3 and Niño 4 indices. Figure 3 thus demonstrates the overall intermittent and uninterrupted representation of CP El Niños throughout 1880 to 2010 in both datasets and methods.

Figure 3(c) summarizes the likelihood of a CP El Niño occurrence through time. It assists with illustrating the years in which the greatest convergence in methods and datasets occurs for classifying CP El Niños. Among others, the following 16 El Niños stand out: 1885/1886, 1914/1915, 1940/1941, 1958/1959, 1963/1964, 1968/1969, 1977/1978, 1986/1987, 1990/1991, 1991/1992, 1992/1993, 1994/1995, 2001/2002, 2002/2003, 2003/2004, and 2004/2005. The convergence in methods and datasets allows these years to be classified as CP events with somewhat greater certainty. Figure 3(c) also exhibits the increased probability of CP El Niños later in the dataset which supports the improved consistency inferred from Fig. 3(a, b). We still see, however, the divergence between different methods and datasets. It is therefore necessary to assess the classification by looking at the anomalous pattern evolution of these individual events (Fig. 4), as they might be misinterpreted by using indices only.

In Fig. 4, the temporal evolution of SSTA is shown as derived from HADISST dataset for the summer June-July-August (JJA), autumn September-October-November (SON), and winter (DJF) seasons. The first impression concerns the general warming tendency from the late nineteenth century to the early twenty-first across the Pacific basin, which is strongest in the latest decades. Three of the initially diagnosed CP El Niño events coincide with the volcanic eruptions of Agung (1963/1964) and Pinatubo (1991/1992 and 1992/1993). To analyze the climatic consequences of

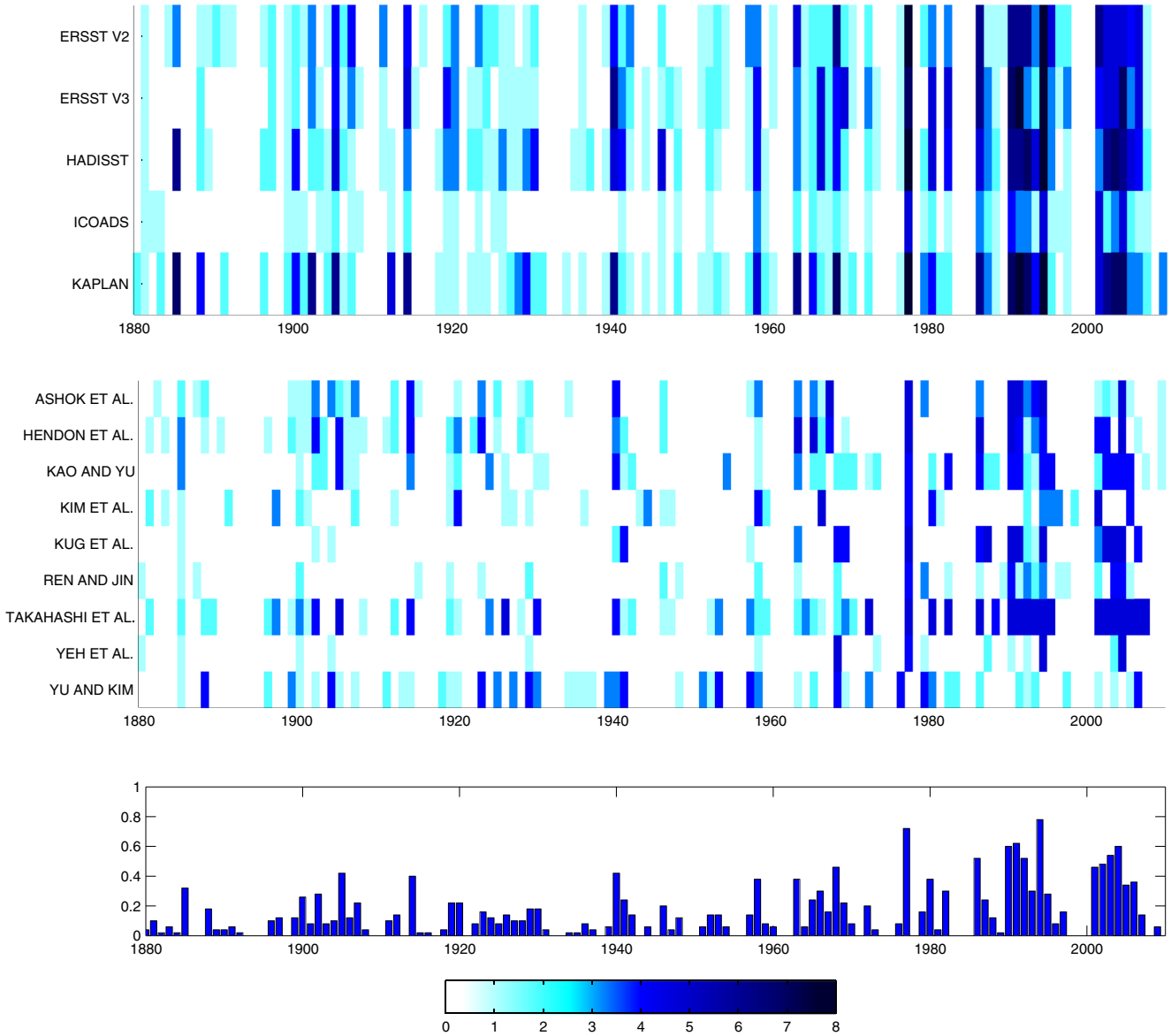

Fig. 3 Number of times a CP El Niño event is classified for each year during the period 1880–2010 according to the methods described in Table 1 (*a*) and datasets (*b*) investigated. Probability that a given year is a CP El Niño year (*c*). The probability (shown on *y-axis*) is calculated by taking the sum of CP events classified for each year in *a* datasets and *b* methods, divided by 45 (i.e., the total possible number of CP events which can occur based on the five datasets and nine methods)

these events, one has to take into account that the stratospheric volcanic aerosol layer might have modulated or even overridden the SST effects (Graf and Zanchettin 2012).

By looking at the mature phase (DJF), we can conclude that three events are misclassified as CP events. Most prominently, this holds for 2001/2002, which clearly is a La Niña event evolving in a generally warmer Pacific background situation, where positive SSTAs are found only in the west of the dateline, but strong negative SSTAs dominate in the east. In 1992/1993, after positive SSTA covering most of the central and eastern tropical Pacific in JJA, a negative anomaly develops along the equator from South America towards the dateline in SON and DJF.

The different evolution patterns of the CP events shown in Fig. 4(a, b) highlight the variable nature of the CP El Niño. It also demonstrates that considering indices alone, even within a multi-index analysis, may result in the misclassification of events. This stresses the need to examine SST patterns, rather than relying on any single index and methodology for classifying CP events.

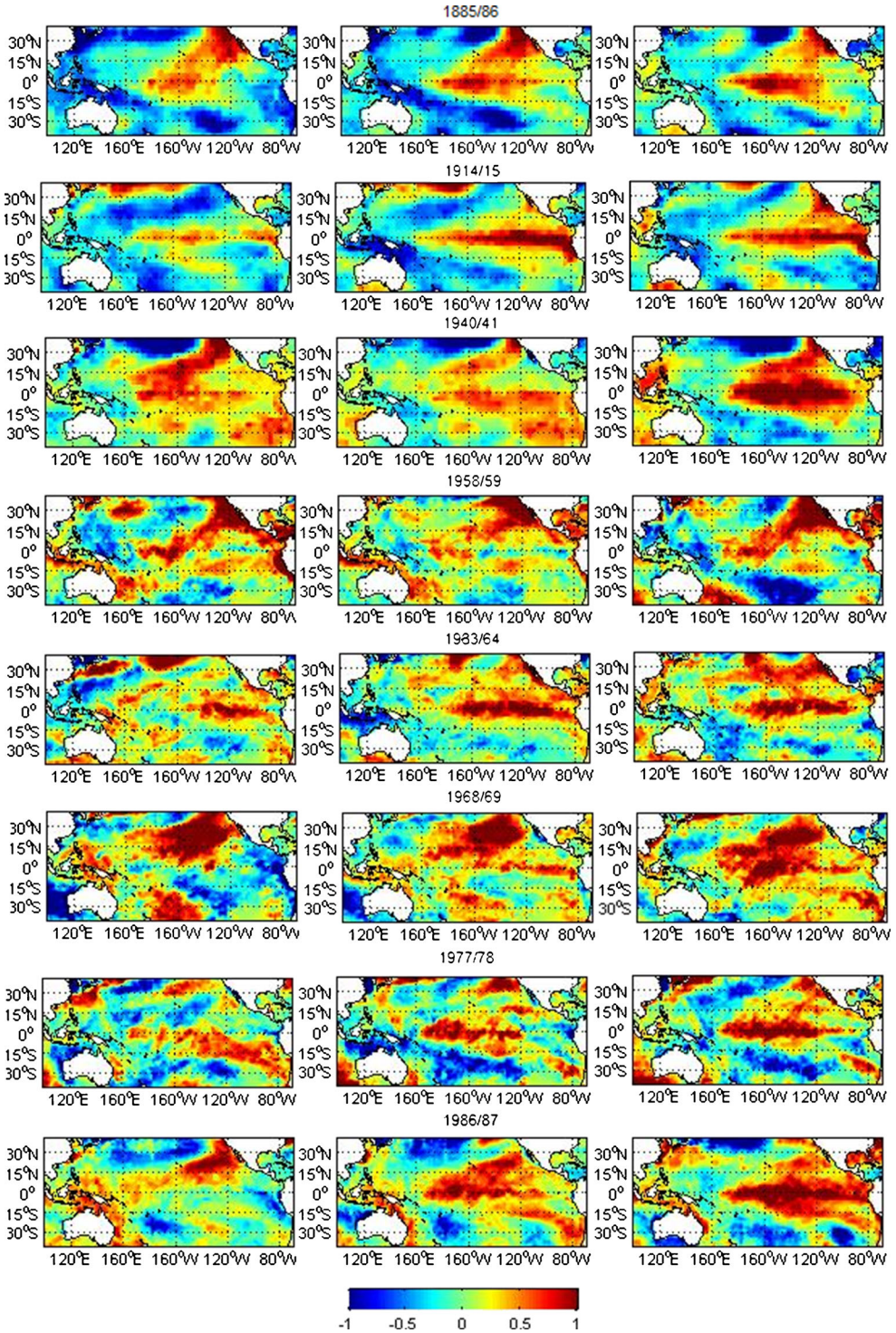

Fig. 4 HadISST SSTA (in degrees Celsius) anomaly maps for the individual CP El Niño events identified in Fig. 3. Maps are shown for the seasons JJA (*left panel*), SON (*middle panel*), and DJF (*right panel*, mature El Niño phase)

Reducing the list of CP events that are obviously misclassified through visual inspection, we find 14 events which may be termed CP El Niño: 1885/1886, 1914/1915, 1940/1941, 1958/1959, 1963/1964, 1968/1969, 1977/1978, 1986/1987, 1990/1991, 1991/1992, 1994/1995, 2002/2003, 2003/2004, and 2004/2005. All these events (except 1914/1915 and 1977/1978) share the common feature of involving

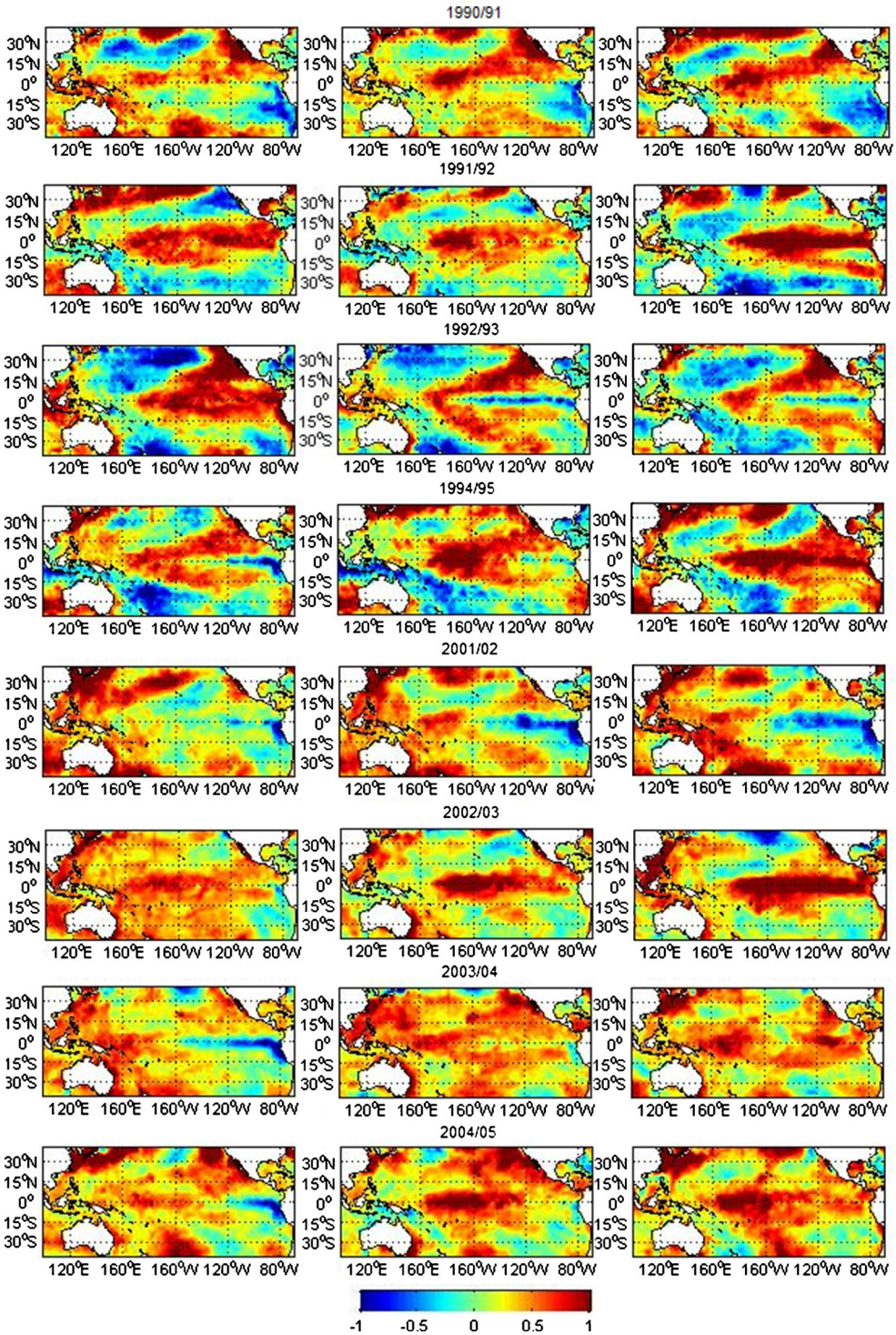

Fig. 4 (continued)

strong positive SSTA off the coast of California and Mexico extending into the Central Pacific in boreal summer (JJA). In the following seasons (SON and DJF), the positive SSTA strengthens and expands near or just east of the dateline, and a slightly negative SSTA appears off the coast of South America.

The pattern correlation statistics (R, where the correlation is performed between each identified CP year and the composite mean) are reported in Table 2. The low correlation of 2001/2002, especially for detrended data, supports the misclassification of this year as determined through visual inspection. Years with the highest R value include 2002/2003,

Table 2 Pattern correlation statistics (R) comparing spatial correlation of the individuated CP El Niño events with the composite CP pattern, for both original and linearly detrended (values in parenthesis) DJF SSTAs from the HadISST dataset. Values are ordered by the value of the detrended R statistic

CP event	R (detrended data)
2002/2003	0.965 (0.963)
1994/1995	0.965 (0.959)
1986/1987	0.920 (0.910)
1940/1941	0.919 (0.915)
1968/1969	0.914 (0.909)
1991/1992	0.897 (0.893)
1914/1915	0.821 (0.877)
2004/2005	0.861 (0.850)
1977/1978	0.850 (0.832)
1963/1964	0.805 (0.806)
1990/1991	0.795 (0.750)
1992/1993	0.789 (0.728)
1885/1986	0.560 (0.710)
1958/1959	0.642 (0.650)
2003/2004	0.681 (0.617)
2001/2002	0.032 (−0.227)

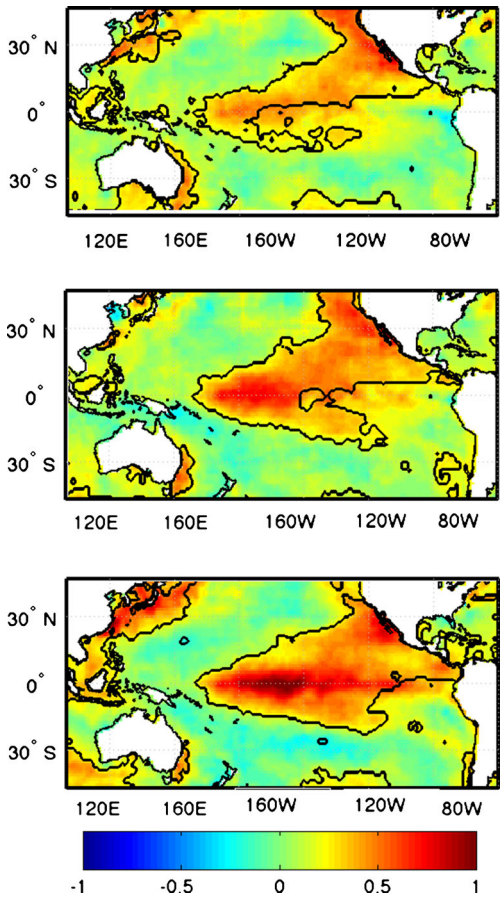

Fig. 5 HadISST SSTA (in degrees Celsius) composite maps of the 14 CP El Niño events identified. Maps are shown for the seasons JJA (*top panel*), SON (*middle panel*), and DJF (*bottom panel*, mature El Niño phase). *Contour* indicates where SSTAs are significant at $p=0.05$, using a two-tailed Student's t test

1994/1995, and 1986/1987. Visual inspection of these years demonstrates a clear Central Pacific SSTA pattern for these years.

Figure 5 shows seasonal composites for these 14 events in the equatorial Pacific (5°N to 5°S, 150°E to 80°W) and also indicates regions where the SSTAs are significant at a 95 % confidence level using a two-tailed Student's t test. These maps demonstrate significant anomalies occurring mostly in the Central Pacific Region, near the areas of the greatest magnitude SSTAs, increasing for the mature season DJF. It is also noted that statistically significant anomalies developed in JJA strengthen and propagate eastwards into SON and DJF.

4 Discussion and conclusions

Through the application of nine different methods taken from the literature to five SST reconstruction/reanalysis datasets, the present study has attempted to constrain the classification of CP El Niño years from 1880 to present. From the results, the following 14 CP events appear with greatest convergence in both the datasets and methods considered: 1885/1886, 1914/1915, 1940/1941, 1958/1959, 1963/1964, 1968/1969, 1977/1978, 1986/1987, 1990/1991, 1991/1992, 1994/1995, 2002/2003, 2003/2004, and 2004/2005. These years are further constrained by an investigation of the HadISST SSTA pattern associated with each individual event (Fig. 4(a, b)). Pattern correlation analysis indicates that the 2002/2003, 1994/1995, and 1986/1987 events most closely resemble the typical CP pattern, while the 2001/2002, 1885/1886, and 1958/1959 events resemble it least. Care should be taken when considering the climate anomalies associated with the 1963/1964 and 1991/1992 CP events which co-occur with volcanic eruptions. Our approach provides a more robust classification of CP El Niños than that permitted by using any method/dataset on its own. These results also show that CP events indeed occur early in the data, though sporadically, contradicting studies claiming it to be a phenomenon exclusive of recent decades (Ashok et al. 2007). The main analysis performed on the original SST data is repeated using linearly detrended SST data to determine the impact of centennial-scale background warming on the classification of CP events. Findings indicate that detrended SST generally increases the likelihood of detecting CP events earlier in the time period for the different datasets/methods but does not change the main result about which events are classified with the greatest convergence. The 14 events classified for the most part demonstrate a pattern of SSTAs which first develops off the coast of South America and Mexico in boreal summer (JJA) which then extends westward toward the Central Pacific.

The occurrence of CP events is also found to persist (though, of course, appearing intermittently) throughout the period 1880–2010. In particular, this is evident when the

methods of Ashok et al. (2007), Hendon et al. (2009), Kao and Yu (2009), and Yu and Kim (2010) are used. The consistency of the CP classifications improves later in the time period, which certainly signals the improvement in the quality and, therefore, convergence between the SST datasets later in the twentieth century. This has also been noted through a comparison of reanalysis and reconstructions in other studies (Giese and Ray 2011; Ray and Giese 2012). The poorer correlation between different datasets earlier in the time period presents a limitation in providing a robust classification prior to 1950. Results are also limited by the discrepancies existing in SSTAs between reconstructions and reanalyses (Deser et al. 2010). Despite this caveat, results from different datasets and indices, nonetheless, classify CP events early in the twentieth century, although individual event years vary.

The occurrence and persistence of CP events from early in the datasets also provides support for studies which identify the CP event as comprising a form of natural climate variability (Newman et al. 2011; McPhaden et al. 2011; Yeh et al. 2011). We note that the period showing prominent CP event clusters after 2000. Periods of CP clusters shown in the SST indices (1900–1910 and 1990–2010) also coincide with the positive phase of the Pacific Decadal Oscillation (PDO, http://www.jisao.washington.edu/pdo/). These patterns are demonstrated further by considering the *C* index (Takahashi et al. 2011) and EMI index (Ashok et al. 2007). The association of ENSO with the PDO has been noted in other studies (e.g., Zhang et al. 1996; Zanchettin et al. 2008). Low-frequency climate variability may therefore be one possible important player in the accumulation of CP events during certain periods.

In conclusion, this study helps to constrain the classification of CP El Niños from the varied approaches which exist in the current literature. There is no classification which could be singled out as the "best." A more robust classification of CP events is necessary to enhance our understanding on their past, present, and future variability, for example, in the application of statistical studies examining their historical prevalence (Nicholls 2008; L'Heureux et al. 2012). The classification method should include information about the physical processes leading to CP events, which differs from canonical EP events (see, e.g., Guilyardi 2006). Our findings have shown that CP events have likely occurred, though only sporadically, in the late nineteenth and early twentieth centuries, and have appeared intermittently throughout the last ~130 years, although with increased frequency during recent decades. Variability in the spatial evolution of the SSTA patterns associated with the CP events was also illustrated, stressing the importance of examining these patterns in addition to relying on indices alone.

Acknowledgments The authors thank Aiko Voigt and an anonymous reviewer for their useful comments on the manuscript. The study also benefitted from critical comments from two anonymous reviewers on an earlier version of this work. MP-C would like to thank the guest program of the International Max Planck Research School on Earth System Modeling (IMPRS-ESM) which made this research possible. DZ and CT acknowledge funding from the Federal Ministry for Education and Research in Germany (BMBF) through the research program "MiKlip" [FKZ: 01LP1158A (DZ)/01LP1130A (CT)]. OB acknowledges funding through the Cluster of Excellence "CliSAP," University of Hamburg, funded through the German Science Foundation (DFG). The authors are grateful to the National Oceanic and Atmospheric Administration Earth System Research Laboratory/Physical Sciences Division for providing their data products at http://www.esrl.noaa.gov/psd/ and the Met Office Hadley Center for providing HadISST data at http://www.metoffice.gov.uk/hadobs/hadisst/.

References

Alexander M, Bladé I, Newman M, Lanzante J, Lau N, Scott J (2002) The atmospheric bridge: the influence of ENSO teleconnections on air–sea interaction over the global oceans. J Climate 15(16):2205

Ashok K, Behera SK, Rao SA, Weng H, Yamagata TJ (2007) El Niño Modoki and its possible teleconnection. J Geophys Res 112: C11007. doi:10.1029/2006JC003798

Deser C, Phillips AS, Alexander MA (2010) Twentieth century tropical sea surface temperature trends revisited. Geophys Res Lett 37: L10701. doi:10.1029/2010GL043321

Feng JA, Wang L, Chen W, Fong SK, Leong KC (2010) Different impacts of two types of Pacific Ocean warming on Southeast Asian rainfall during boreal winter. J Geophys Res 115:D24122. doi:10.1029/2010JD014761

Giese BS, Ray S (2011) El Nino variability in simple ocean data assimilation (SODA), 1871–2008. J Geophys Res 116:C02024. doi:10.1029/2010JC006695

Graf H-F, Zanchettin D (2012) Central Pacific El Niño, the "subtropical bridge" and Eurasian Climate. J Geophys Res 117:D01102. doi:10.1029/2011JD016493

Guilyardi E (2006) El Niño-mean sate-seasonal cycle interactions in a multi-model ensemble. Clim Dyn 26(4):329–348. doi:10.1007/s00382-005-0084-6

Hendon HH, Lim E, Wang GM, Alves O, Hudson D (2009) Prospects for predicting two flavors of El Niño. Geophys Res Lett 36:L19713. doi:10.1029/2009GL040100

Kao H-Y, Yu J-Y (2009) Contrasting Eastern-Pacific and Central-Pacific types of ENSO. J Climate 22:615–632 doi:10.1175/5112008JCLI2309.1

Kaplan A, Cane M, Kushnir Y, Clement A, Blumenthal M, Rajagopalan B (1998) Analyses of global sea surface temperature 1856–1991. J Geophys Res 103:18,567–18,589. doi:10.1029/97JC01736

Kim ST, Yu J-Y (2012) The two types of ENSO in CMIP5 models. Geophys Res Lett. doi:10.1029/2012GL052006

Kim H, Webster PJ, Curry JA (2009) Impact of shifting patterns of Pacific Ocean warming on north Atlantic tropical cyclones. Science 325(5936):77–80. doi:10.1126/science.1174062

Kug J-S, Jin FF, An S-I (2009) Two types of El Niño events: cold tongue El Niño and warm pool El Niño. J Climate 22:1499–1515. doi:10.1175/2008JCLI2624.1

L'Heureux M, Collins D, Hu Z-Z (2012) Linear trends in sea surface temperature of the tropical Pacific Ocean and implications for the El Niño-Southern Oscillation. Clim Dyn 1–14. doi:10.1007/s00382-012-1331-2

Larkin NK, Harrison DE (2005) On the definition of El Niño and associated seasonal average U.S. weather anomalies. Geophys Res Lett 32:L13705. doi:10.1029/2005GL022738

Lee T, McPhaden MJ (2010) Increasing intensity of El Niño in the central-equatorial Pacific. Geophys Res Lett 37. doi:10.1029/2010GL044007

Lian T, Chen D (2012) An evaluation of rotated EOF analysis and its application to tropical pacific SST variability. J Climate. doi:10.1175/JCLI-D-11- 00663

McPhaden MJ, Lee T, McClurg D (2011) El Niño and its relationship to changing background conditions in the tropical Pacific Ocean. Geophys Res Lett 38:L15709. doi:10.1029/2011GL048275

Newman M, S-I Shin, Alexander MA (2011) Natural variation in ENSO flavors. Geophys Res Lett 38:L14705. doi:10.1029/2011GL047658

Nicholls N (2008) Recent trends in the seasonal and temporal behaviour of the El Niño Southern Oscillation. Geophys Res Lett 35(L19703). doi:10.1029/2008GL034499

Rasmusson EM, Carpenter TH (1982) Variation in tropical sea surface temperature and surface wind fields associated with Southern Oscillation/El Niño. Mon Weather Rev 110:354–384

Ray S, Giese BS (2012) Historical changes in El Nino and La Nina characteristics in an ocean reanalysis. J Geophys Res 117:C11007. doi:10.1029/2012JC008031

Rayner NA, Parker DE, Horton EB, Folland CK, Alexander LV, Rowell DP, Kent EC, Kaplan A (2003) Global analyses of sea surface temperature, sea ice, and night marine air temperature since the late nineteenth century. J Geophys Res 108:D144407. doi:10.1029/2002JD002670

Ren H, Jin F-F (2011) Niño indices for two types of ENSO NIÑO indices for two types of ENSO. Geophys Res Lett 2011–02;38:n-a-n/a

Smith TM, Reynolds RW (2004) Improved extended reconstruction of SST (1854–1997). J Climate 17:2466–2477. doi:10.1175/1520-0442

Smith TM, Reynolds RW, Peterson TC, Lawrimore J (2008) Improvements to NOAA's historical merged land-ocean surface temperature analysis (1880–2006). J Climate 21:2283–2296. doi:10.1175/2007JCLI2100.1

Takahashi K, Montecinos A, Goubanova K, Dewitte B (2011) ENSO regimes: reinterpreting the canonical and Modoki El Niño. Geophys Res Lett 38:L10704. doi:10.1029/2011GL047364

Trenberth KE, Hoar TJ (1997) El Niño and climate change. Geophys Res Lett 24(23):3057–3060. doi:10.1175/1520-0477(1997)078<2771:TDOENO>2.0.CO;2

Trenberth KE, Stepaniak DP (2001) Indices of El Niño evolution. J Climate 14(8):1697–1701. doi:10.1175/1520-0442(2001)014<1697:LIOENO>2.0.CO;2

Walker GT (1923) Correlation in seasonal variations of weather. III: a preliminary study of world weather. Mem Indian Meteor Dept 24:75–131

Walker GT (1924) Correlation in seasonal variations of weather. IV: a further study of world weather. Mem Indian Meteor Dept 24:275–332

Worley SJ, Woodruff SD, Reynolds RW, Lubker SJ, Lott N (2005) ICOADS release 2.1 data and products. Int J Climatol 25:823–842

Yeh S, Kug J, Dewitte B, Kown M-H, Kirtman BP, Jin F-F (2009) El Niño in a changing climate. Nature 461(7263):511–U70. doi:10.1038/nature08316

Yeh S-W, Kirtman BP, Kug J-S, Park W, Latif M (2011) Natural variability of the central Pacific El Niño event on multi-centennial timescales. Geophys Res Lett 38:L02704, doi:10.1029/2010GL045886

Yu J, Kim ST (2010) Identification of Central-Pacific and Eastern-Pacific types of ENSO in CMIP3 models EP AND CP ENSO IN CMIP3 MODELS. Geophys Res Lett 2010-08;37:n-a-n/a

Zanchettin D, Franks SW, Traverso P, Tomasino M (2008) On ENSO impacts on European wintertime rainfalls and their modulation by the NAO and the Pacific multidecadal variability described through the PDO index. Int J Climatol 28:995–1006. doi:10.1002/joc.1601

Zhang Y, Wallace JM, Battisti DS (1996) ENSO-like interdecadal variability: 1900–93. J Climate 10:1004–1020. doi:10.1175/1520-0442(1997)010<1004:ELIV>2.0.CO;2